Synergistic effect between oxides semiconductors and zeolites on photobleaching of RB250 textile dye

Jean César Marinozi Vicentini[*], Gabriela Brunosi Medeiros, Maria Clara Chimirri Watanabe, Karen Raiane Piccoli, Fernanda Carla Camilo and Mara Heloisa Neves Olsen Scaliante

*Departamento de Engenharia Química, Universidade Estadual de Maringá, Avenida Colombo, 5790, 87020-900, Maringá, Paraná, Brazil. *Author for correspondence. E-mail: jcmarinozi@gmail.com*

ABSTRACT. The present work aims to evaluate the activity of semiconductor oxides (TiO_2, Nb_2O_5 and ZnO) supported on NaA and NaY zeolites, as well as their synergistic effect on Reactive Blue Dye (RB250) photodegradation process. Prior to deposition, TiO_2 particles size was reduced by ultrasonic scattering followed by filtration. The particles on the filtrate were used to conduct the experiments. The semiconductors were immobilized in concentrations of 2.5, 5 and 10% (w w^{-1}) and the photocatalytic tests were performed at catalyst concentrations of 1 and 2 g L^{-1}. Moreover, supported catalysts were characterized by XRD, textural analysis, zero point of charge and temperature programmed desorption of NH_3. A comparison between the supported catalysts showed high activity for the ones supported with ZnO and TiO_2. Zeolite NaY has broader opened channels than NaA, which reduces the dye molecules blockage, and, as a result, increased the catalyst activity. A higher concentration of supported catalysts (2 g L^{-1}) provides greater photocatalytic activity, while higher concentration of semiconductors immobilized on supports does not present significant differences.

Keywords: NaA; NaY; TiO_2; Nb_2O_5; ZnO; AOPs.

Efeito sinérgico entre óxidos semicondutores e zeólitas no fotoclareamento do corante têxtil RB250

RESUMO. O objetivo deste trabalho foi avaliar a atividade dos óxidos semicondutores (TiO_2, Nb_2O_5 & ZnO) suportados nas zeólitas NaA e NaY e seu efeito sinérgico na fotodegradação do corante têxtil azul reativo (RB250). Antes da deposição, o tamanho das partículas de TiO_2 foi reduzido por dispersão em ultrassom seguido por filtração e foram utilizadas as partículas que passaram através do filtro. Os semicondutores foram imobilizados em concentrações de 2,5, 5 e 10% (m m^{-1}) e os testes fotocatalíticos foram realizados em concentrações de catalisador de 1 e 2 g L^{-1}. Os catalisadores suportados foram caracterizados por DRX, análise textural, ponto de carga zero e dessorção por temperatura programada. Os catalisadores suportados com ZnO e TiO_2 mostraram maior atividade do que o Nb_2O_5. Os testes fotocatalíticos indicaram um aumento na atividade dos catalisadores suportados em NaY sendo essa com resultados superiores aos encontrados com a zeólita NaA. Isso por causa dos seus canais mais estreitos que dificultam a entrada de moléculas do corante. A maior concentração de catalisadores suportados (2 g L^{-1}) proporciona maior atividade fotocatalítica, enquanto a maior concentração de semicondutores imobilizados em suportes não apresenta diferenças significativas.

Palavras-chave: NaA; NaY; TiO_2; Nb_2O_5; ZnO; AOPs.

Introduction

According to the United Nations Educational World, Scientific and Cultural Organization (Unesco, 2015), the water consumption increases two times faster than the population. As a result, the demand of water resources will increase 55% until 2050. Textile industries are major consumers of water and fuel, once around of 50% of their costs are on fibers washing and wastewater (Mohsin, Rasheed, Farooq, Ashraf, & Shah, 2013). Among the dyes diversity, the reactive ones are detectable at concentrations above 5 μg L^{-1} (Brites-Nóbrega, Santana, & Fernandes-Machado, 2011). Even though the concentration is low, it could block the light penetration, unbalancing the aquatic ecosystem and exhibiting a high BOD and COD load (Smith, 2003).

Adsorption and coagulation processes have good efficiency in removing pollutants from water, just like filtration. However, those techniques generate secondary pollutants, which needs post treatments or specific destinations (Gaya & Abdullah, 2008), increasing the time operation and the process cost.

Nowadays, advanced oxidation processes (AOPs) have been successfully used in wastewater treatment field (Soon & Hameed, 2011). AOPs can provide a complete mineralization of pollutants from water into innocuous compounds, such as hydrolysis products of water and mineral acids, eliminating those pollutants and avoiding the generation of new contaminants (Liotta, Gruttadauria, Di Carlo, Perrini, & Librando, 2009).

Among the photocatalysis advantages, its applicability at room temperature and the activation with light energy (sunlight or artificial) stands (Chong, Jing, Chow, & Saint, 2010). Several examples of the application of photocatalysis have been reported in the literature, proving that the referred process accelerates the reaction of the water hydrolysis and favors the transient radical's generation. The lower operation time required in a photocatalytic plant reduces about 60% of the estimated procedure costs, due to the energy consumption (Prado, Bolzon, Pedroso, Moura, & Costa, 2008; Chong et al., 2010). Furthermore, TiO_2 is one of the most active photocatalysts studied due to its stability under adverse temperature and pH conditions (Chong et al., 2010). ZnO also has optimum efficiency in the mineralization of organic compounds. In contrast, Nb_2O_5 causes the formation of unstable hydrocolloid in water, which causes the catalyst precipitation and makes its separation easier. However, the precipitation avoids the light absorption from catalysts (Chong et al., 2010; Brites-Nóbrega et al., 2011).

Zeolites are strong candidates for catalyst supports, due to their characteristics, such as stability, high pore volume, adsorbent property and homogeneous pore structure. Those characteristics contribute for the supported catalyst porosity and mechanical resistance (Augugliaro, Litter, Palmisano, & Soria, 2006). Zeolites A and Y are both microporous and have crystalline cubic structure, differing only in Si/Al inter-reticular ratio. While Zeolite NaA have the Si/Al ratio equal to 1, zeolite NaY have Si/Al ratio higher than 1.5. Thus, that indicates a higher proton acidity for zeolite NaA (Petkowicz, Pergher, Rochac, & Santos, 2010). Despite the low Si/Al ratio on zeolites NaA, they also have photocatalytic activity. That is because the hydrophilic surface favors the formation of hydroxyl radicals by the photoactivation and the hydrolysis of the surface adsorbed water (Brites-Nóbrega et al., 2015).

Even though the immobilization of TiO_2 on supports can increase the mass transfer limitations, reducing the photocatalytic activity, it prevents catalyst loss by leaching and allows the catalyst

recycles (Hadjltaief, Zina, Galvez, & Costa, 2016). The key parameters in a photocatalytic test are the active phase concentration on the support surface and the optimal concentration of the supported catalyst. Those parameters indicate the highest photocatalytic efficiency for a particular catalyst with low procedure costs (Nikazar, Gholivand, & Mahanpoor, 2008; Fan, Guo, Wang, & Fan, 2009). Thus, the consolidation of photocatalysis in the wastewater treatment field is strongly dependent on the development of appropriate catalysts.

By comparing the activities of two types of support and evaluating the activity of the suspended and immobilized metal oxide, the synergistic effect between catalyst and support is verified. ZnO/NaX and ZnO/activated coal were prepared in order to verify the synergistic effect between oxide and support in the reactive blue dye 5G photomineralization activity (Brites-Nóbrega et al., 2013). Due to the acidic surface characteristics of NaX catalyst, which allows greater electronic excitation, the authors observed that the metal oxide presented a higher interaction with the zeolite when compared to the activated coal. That is because the activated coal catalyst blocked the acidity introduced by the oxides. Moreover, the dye degradation was less effective (98%) when ZnO evaluated in suspension than when immobilized on NaX (100%). These results confirm the synergistic effect introduced by the support on the supported catalyst (Brites-Nóbrega et al., 2013).

This work aims to evaluate the photocatalytic activity and kinetic for different metal oxides (TiO_2, Nb_2O_5 and ZnO), supported at different concentrations on zeolites NaA and NaY, for photodegradation of reactive blue dye (RB250) under UV irradiation. In addition, the synergistic effect between the active phases and zeolite supports were not mentioned on the literature before and will be discussed on the present study.

Material and methods

Materials

The chemicals used were: oxalic acid (Nuclear 0.5 mol); zinc nitrate (dynamic P.A.); niobic acid (HY-340 CBMM with 76.2% Nb_2O_5); titanium dioxide (Kronos 100% Anatase); NaOH (Vetec); HNO_3 (Vetec), reactive blue dye (RB250 - Donated by Sintex dyeing) and Zeolites NaA and NaY.

Catalyst preparation

The immobilized catalyst with 2.5% of active phase (ZnO or Nb_2O_5) was prepared by wet impregnation method (Brites-Nóbrega et al., 2011). The immobilized catalyst with Nb_2O_5 were prepared by

adding 1 g of the niobic acid in 34.3 mL of oxalic acid solution, at 70°C for 24 hours. For ZnO catalysts, the precursor salt used was an aqueous solution of zinc nitrate. Prior to the addition of Nb_2O_5 (or ZnO) on the zeolitic support (NaA or NaY), the zeolites were dried at a temperature of 100°C for 24 hours. The solvent removal was performed in a rotary vacuum evaporator. Then, the solid was calcined at 500°C for 5 hours. The supported catalysts prepared, 2.5% ZnO/NaY; 2.5% Nb_2O_5/NaY, 2.5% ZnO/NaA and 2.5% Nb_2O_5/NaA were taken to the oven for 24 hours.

Catalysts supported with TiO_2 metal oxide were prepared by physical deposition method, in which the commercial TiO_2 was dispersed in deionized water in proportions of 2.5, 5 and 10% (w w^{-1}) with zeolite A or zeolite Y, previously dried at a temperature of 100°C for 24 hours. The mixture was kept under stirring until its complete homogenization. After that the solvent was removed on a rotatory vacuum evaporator. For supported catalysts with reduced particles of TiO_2 the immobilization was by physical deposition either. To produce TiO_2-reduced catalyst, TiO_2 particles passed through a size reduction process before the deposition. Initially, the commercial TiO_2 was dispersed in water under ultrasound and, then, filtered through 3 μm hydrophilic membrane. The filtrate was dried and used in subsequent deposition. The catalysts prepared were 2.5% TiO_2/NaY; 5.0% TiO_2/NaY; 10% TiO_2/NaY; 2.5% TiO_2/NaA and 2.5% TiO_2-reduced/NaY. The catalysts were calcined at 500°C for 5 hours.

After the heat treatment, all the prepared catalysts prepared were characterized and subsequently applied to photocatalysis tests.

Photocatalytic tests

The photocatalytic tests were carried out on a reactor filled with 500 mL of 10 mg L^{-1} dye solution and catalyst concentration of 1 and 2 g L^{-1}, for 5 hours under irradiation (the analysis were performed in duplicate). The reactor was equipped with a magnetic stirrer and the temperature was controlled at 25°C. The radiation was provided by a 250 W lamp (Empalux) without bulb for UV radiation. Aliquots were taken at regular intervals of 1 h and filtered with Millipore membranes (0.22 μm). The absorbance of each aliquot was measured at 617nm for evaluation of the catalytic activity. The percentage of dye discoloration was calculated by Equation 1:

$$Decoloration\ (\%) = \frac{(C_i - C) \times 100}{C_i} \qquad (1)$$

Where C_i is the initial concentration of dye and C is the dye concentration after 5 hours of irradiation.

Considering it is a photocatalytic reaction, the reagents and radicals present in the solution adsorb on the catalyst surface by Langmuir-Hinshelwood mechanism.

According to Brites-Nóbrega et al. (2011), Nikazar et al. (2008) and Ejhieh and Khorsandi (2010), the chemical kinetic reactions of organic compounds photo-oxidation in aqueous solution follow the model proposed by Langmuir-Hinshelwood (Equation 2).

$$r = -\frac{dC}{dt} = \frac{kKC}{1 + KC} \qquad (2)$$

where:
k is the kinetic constant and K is the adsorption constant.

When the solution is diluted for concentrations below 50 mg L^{-1}, the rate law can be simplified with $KC << 1$ (Brites-Nóbrega et al., 2011). After the simplification and integration with Equation 1, the Equation 3 is obtained.

$$ln\left(\frac{C_i}{C}\right) = k \times t \qquad (3)$$

The half-life time of the reaction is calculated by the Equation 4.

$$t_{1/2} = \frac{Ln\ 2}{k} \qquad (4)$$

where:
t is the irradiation exposure time and $t_{1/2}$ is the half-life time.

Characterization

The textural properties of catalysts such as specific surface area, micropore volume and micropore mean diameter were determined by physical adsorption isotherms of N_2 using Quantachrome NOVA 1200 apparatus. The X-ray patterns diffraction (XRD) was performed using an X-ray diffractometer Bruker D8 Advance 2θ from 5 to 85°, CuKα radiation, 0.24° min^{-1} and 40 kV. The proton acidity was determined by Temperature Programmed Desorption of NH_3 (TPD) in Chembet 3000 Quantachrome Instruments coupled with spectrometer Pfeiffer Vacum. The point of zero charge (pHzpc) of the supported catalysts, in terms of the pH of the suspension (Equation 5), was measured by a pH meter pH Meter Tecnal Tec-2 (Gillman & Uehara, 1980).

$$pH_{ZPC} = 2pH_{KCL} - pH_{H_2O} \qquad (5)$$

Results and discussion

Textural analysis

The textural parameters had a large decrease after the deposition and impregnation of metal oxides on zeolite NaA (Table 1). The reduction in the BET total surface area indicates that there was an almost complete occupation of the zeolite surface. For the surface micropore area and micropore volume was observed that there was a complete obstruction of the pores by the immobilized material. The increase in the pore diameter should be by cluster of the active phase on the zeolite surface resulting in erroneous increase of the pore diameter of the supported catalyst.

Table 1. Textural parameters from zeolitic supports and supported catalysts. 'S_{BET}' is the total surface area, 'S_{micr}' is the micropore surface area, 'V_{micr}' is the micropore volume and 'D_p' the pore diameter.

Catalysts	$S_{BET}{}^a$ (m² g⁻¹)	S_{micr} (m² g⁻¹)	V_{micr} (cm³ g⁻¹)	D_p (Å)
NaY	451	443	0,34	4.0
NaA	51.0	36.0	0.02	8.8
2.5% TiO₂/NaA	5.00	0.00	0.00	17
2.5% ZnO/NaA	6.00	0.30	0.00	16
2.5% Nb₂O₅/NaA	7.00	0.50	0.00	18
2.5% TiO₂/NaY	628	589	0.31	5.2
5.0% TiO₂/NaY	625	579	0,28	4.9
10% TiO₂/NaY	599	552	0.27	5.2
2.5% ZnO/NaY	729	680	0.32	4.2
2,5% Nb₂O₅/NaY	663	609	0.30	5.3
2.5% TiO₂-reduced/NaY	618	566	0.30	5.4

^{a}(0.1 ≤ P/P₀ ≤ 0.3).

The increase in BET total surface area and micropore surface area with semiconductors supported on zeolite NaY indicates that there was loss of amorphous material during the preparation of the catalysts. Probably the NaY zeolite had amorphous material in its structure and during catalyst preparation this material could have been leached. The BET method is not effective in quantifying the textural parameters of zeolites because zeolite pores are smaller than the kinetic diameter of N₂ molecule (Brek, 1976).

X-ray diffraction

The X-ray diffraction patterns for supported catalysts were carried out with the aim to identify the crystalline phases present in the samples. The diffraction patterns were analyzed using the database ICDD PDF2 (Philips) Software Xpert Score.

It has been found that methods for obtaining supported catalysts preserved all the characteristics of the zeolites structures when compared to the initial NaA and NaY diffractograms. It was not possible to identify the peaks relating to the active phase in the diffraction lines of the catalysts due to the low concentration of metal oxide on support surface (Figure 1a, b and c).

A reduction in crystallinity was identified by reduction of intensity peaks (Figure 1a and b) of supported catalysts compared with the XRD pattern of the pure zeolite due to the good dispersion of the active phase on the zeolites supports. The increase of the intensity peaks in Figure 1b may be due to the loss of amorphous material during the catalyst preparation from NaY supported catalysts, as seen on textural parameters.

It was also observed that an increasing of the metallic oxide concentration on zeolite surface decreases the crystallinity of the peaks 2θ equal to 6.3; 10.1; and 11.9° (Figure 1c). The reduced crystallinity, compared between the samples 2.5% TiO₂-reduced/NaY and 2.5% TiO₂/NaY, can be explained by the clogging pores, as identified by textural analysis. That also causes the reduction in size of the TiO₂ particle after ultrassound dispersing treatment. These particles were analyzed at an optical microscopic and their size were between 1.0 and 2.0 μm. The size reduction from TiO₂ was approximately 16%, from 870 to 738 nm, by Sherrer equation (Schmal, 2011).

Point of zero charge

The point of zero charge (pH$_{PCZ}$) is an important information because it features one of the adsorption limiting factors. When the pH of the reaction medium is higher than the pH$_{PCZ}$, the catalyst surface adopts positive charges due to the adsorption of the H⁺ ions. When the solution pH is below pH$_{PCZ}$, the desorption of H⁺ or adsorption of OH⁻ occurs and characterize the negative surface charge (Kosmulski, 2011).

The pH of the dye solution is around 6.0. Thus, catalysts that present pH$_{PCZ}$ different from the pH of the dye solution will cause surface charge instability. This instability will favor the dye adsorption on the surface by electrostatic forces.

As noted on Table 2, TiO₂ and Nb₂O₅ presented pH$_{PCZ}$ values near the region highlighted in the literature (Prado et al., 2008; Kosmulski, 2011). ZnO, in the literature, presents a pH$_{PCZ}$ in the range of 8.9. That indicates that the oxide preparation method may have influenced the pH$_{PCZ}$ value (Sędłak & Janusz, 2008). It was also notable a reduction in the point of zero charge for TiO₂-reduced compared with commercial TiO₂. That can be explained by the reduction in crystallite size, as seen in a similar case by Sędłak and Janusz, (2008).
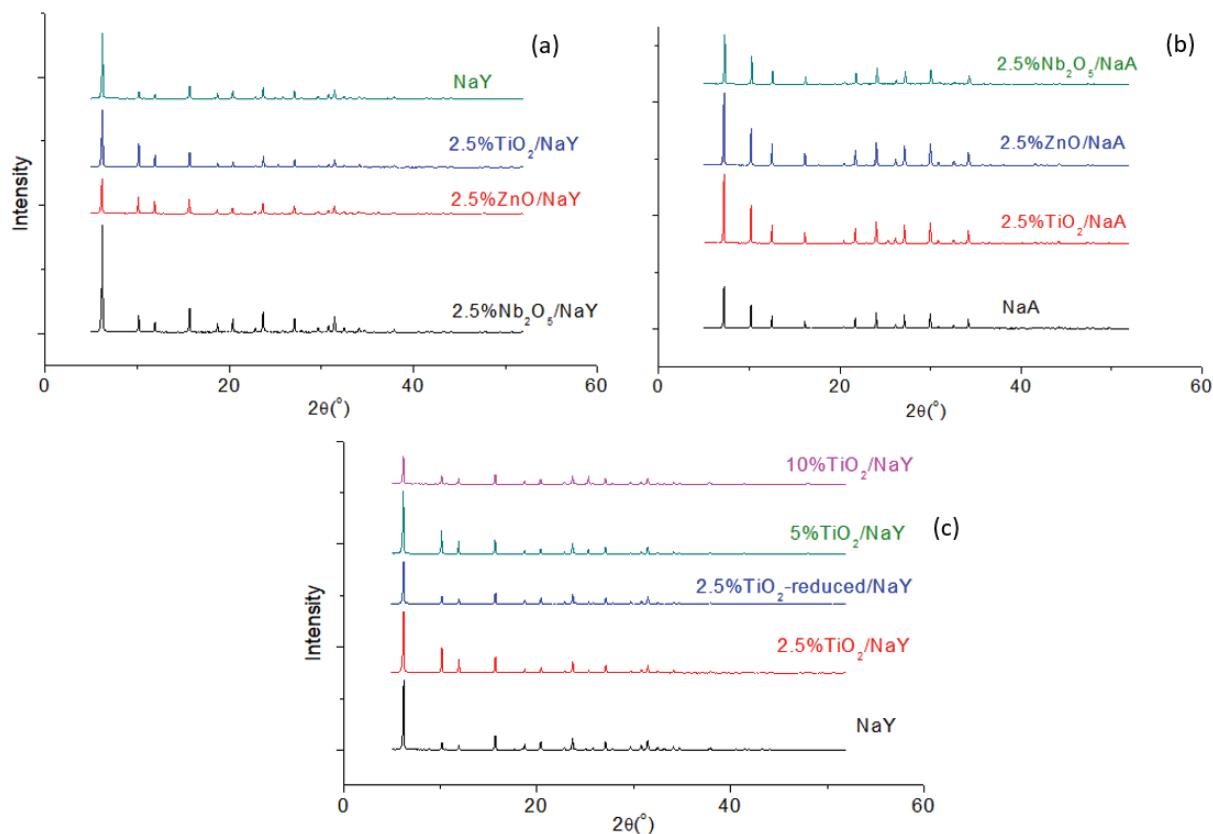
Figure 1. XRD patterns from catalysts supported on (a) NaY (b) NaA (c) XRD patterns from TiO$_2$ supported on NaY zeolite in different concentrations.

Table 2. Point of zero charge (pH$_{PCZ}$) and proton acidity (mmol NH$_3$ g^{-1} catalyst) from zeolitic supports and supported catalysts.

Catalysts	pH$_{PCZ}$	mmol NH$_3$ g$_{catalyst}^{-1}$
NaY	6.9	0.039
NaA	5.4	1.395
TiO$_2$	6.1	0.297
TiO$_2$-reduced	5,0	0.285
ZnO	6.0	0.058
Nb$_2$O$_5$	4.4	0.013
2.5% TiO$_2$/NaA	5.0	1.481
2.5% TiO$_2$-reduced/NaY	5.0	0.631
2.5% Nb$_2$O$_5$/NaA	7.9	1.270
2.5% ZnO/NaA	3.8	1.328
2.5% TiO$_2$/NaY	7.0	0.824
5.0% TiO$_2$/NaY	7.1	0.857
10% TiO$_2$/NaY	6.9	0.683
2.5% ZnO/NaY	6.1	0.817
2.5% Nb$_2$O$_5$/NaY	5.9	1.329

Temperature programmed desorption of NH$_3$

The proton acidity is an important property for zeolites. This property defines how hydrophilic or hydrophobic zeolite is. Higher Al atoms or lower Si/Al ratio, increase the zeolites proton acidity and the hydrophilicity. According to Kosinov, Auffret, Borghuis, Sripathi, and Hensen (2015), zeolites with hydrophilic characteristics contributes to greater activity in the removal of organics from water, while zeolites with hydrophobic characteristics are attributed to the recovery of organics from water.

NaA zeolite has higher acidity compared to the NaY zeolite. Zeolite A has higher Si/Al ratio than zeolite Y, which leads to the formation of narrower channels on NaA than on NaY zeolite. As a result, that makes difficult the NH$_3$ desorption, moving the desorption peaks to higher temperature. Moreover, it was found an increase in proton acidity for catalysts supported on NaY after impregnation of metal oxide (Table 2). This increase was due to non-stoichiometric metal impregnation, which results in decompensation of surface charges due to removal of the Na$^+$ compensation cation. The cation compensation removal was attributed to the difference between the pH of the immobilization step and pH$_{PCZ}$ from zeolitic supports (Giannetto, Rendón, & Fuentes, 2000). The major increase in acidity of Nb$_2$O$_5$ supported on NaY is due to their strongly acidic characteristics in comparison with TiO$_2$ and ZnO (Prado et al., 2008).

Dye photo-decoloration

For the catalyst supported on NaA zeolite (Figure 2b), all the metal oxides applied had a photocatalytic activity very close, but low

photobleaching, when compared to NaY catalysts, were observed in the photocatalytic tests. Even though the proton acidity of the catalyst supported on NaA is greater than NaY zeolite, the low photoactivity is explained by its narrower channels that hinder the entry of dye molecules. The low textural parameters values indicate a poor distribution of oxide over the surface, disfavoring the adsorption of the dye and the light absorption by the metal oxide.

Applying the supported catalysts (oxide/NaA) on concentration of 2 g L^{-1}, the tests resulted in a higher photodegradation activity (Figure 2c) when compared with the tests performed with a concentration of 1 g L^{-1} (Figure 2b). Figure 2c also shows that TiO_2 and ZnO catalyst supported on NaA have the best results. The catalyst 2.5% Nb_2O_5/NaA kept low activity in photodegradation of RB250 dye, even at higher concentration.

The higher concentrations of TiO_2 supported on NaY provides greater active phase area, as a result, it would give a greater photocatalytic activity. The catalyst 10% TiO_2/NaY gives a higher photoactivity with a slight difference between the catalysts with low concentration (Figure 2d). This difference, when compared to the 2.5% TiO_2/NaY, indicates the non-necessity of using high active phase concentrations.

The catalyst 2.5% TiO_2-reduced/NaY was prepared by using TiO_2 with ultrasound size reduction and it did not improved the photodegradation process. However, it showed low activity when compared with the 2.5% TiO_2/NaY catalyst. Some reasons for that are the lower textural parameters and the possibility of reduced particle size oxide occupy the interior of the zeolite channels and not be photo-activated.

In the first adsorption time, the catalyst 2.5% TiO_2/NaY adsorbed a small amount of the reagents and radicals. It was caused by the low active phase area, high zeolitic surface and the distance from the pHPCZ to the solution pH. As a result, the adsorption is favored by the unbalanced charge between the surface and the solution.

Table 3 shows that the most effective system for the degradation of dye solution was the catalyst 2.5% TiO_2/NaY applied with a concentration of 2 g L^{-1}, once it had the highest kinetic constant, and, consequently, the shorter half-life time. When studying the support interference on the degradation activity, it is concluded that the zeolite NaY offers better textural parameters and greater absorption of radiation.

Table 3. Kinetic parameters from photocatalytic tests 'k' is the kinetic constant and 'τ' the half-life time.

Catalysts	k (hour^{-1})	$\tau_{1/2}$ (hour)
2.5% TiO_2/NaA (1 g L^{-1})	0.0685	4.4
2.5% ZnO/NaA (1 g L^{-1})	0.0634	4.7
2.5% Nb_2O_5/NaA (1 g L^{-1})	0.0642	4.7
2.5% TiO_2/NaA (2 g L^{-1})	0.2898	1.0
2.5% ZnO/NaA (2 g L^{-1})	0.1510	2.0
2.5% Nb_2O_5/NaA (2 g L^{-1})	0.0547	5.5
2.5% TiO_2/NaY (1 g L^{-1})	0.0994	3.0
5.0% TiO_2/NaY (1 g L^{-1})	0.0840	3.6
10% TiO_2/NaY (1 g L^{-1})	0.1089	2.8
2.5% ZnO/NaY (1 g L^{-1})	0.1777	1.7
2.5% Nb_2O_5/NaY (1 g L^{-1})	0.1067	2.8
2.5% TiO_2-reduced/NaY (1 g L^{-1})	0.0722	4.2
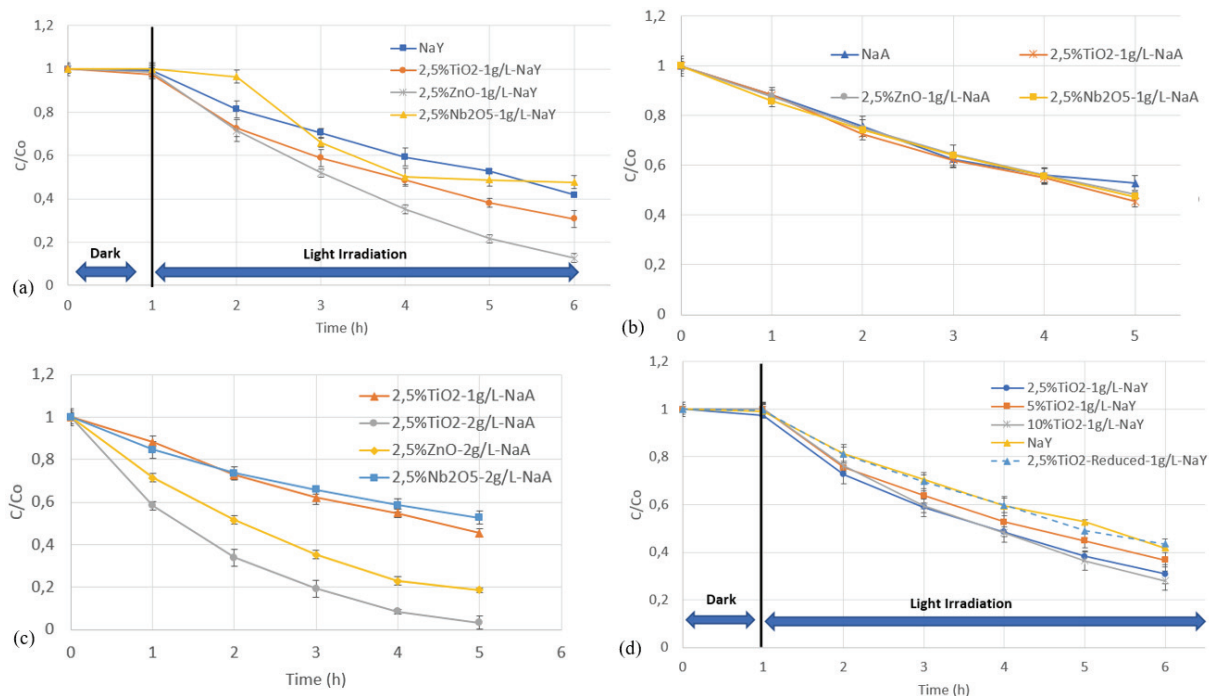
Figure 2. Photocatalytic tests from supported catalysts on (a) NaY (b) NaA (c) NaA applied on 2 g L^{-1} (d) Photocatalytic tests from TiO_2 types supported on NaY.

Conclusion

The immobilization of metal oxides in the zeolite NaA is associates with a reduction of the catalyst textural parameters, indicating an irregular metal occupation on the zeolite surface. An increase on parameters was observed for catalysts supported on NaY, caused by the loss of amorphous material during the steps of the immobilized catalysts synthesis. In the photocatalytic tests, it was observed that the greatest activity was independent of the TiO_2 concentration, followed by ZnO and Nb_2O_5. The grained TiO_2 introduces minor efficiencies when compared to the initial TiO_2. When the system with 2 g L^{-1} catalyst concentration were used, the degradation enhanced because of the better distribution of the active phase solution on the support. Therefore, the photocatalytic applications are very promising since they provide high efficiency, low cost, low operation time and no secondary pollutants formation. Our research group has some papers published in congress proceedings (COBEQ, EAIC and SEQ) that include studies similar to the present.

Acknowledgements

References

Augugliaro, V., Litter, M., Palmisano, L., & Soria, J. (2006). The combination of heterogeneous photocatalysis with chemical and physical operations: A tool for improving the photoprocess performance. *Journal of Photochemistry and Photobiology C: Photochemistry,* 7(4), 127-144. doi: 10.1016/j.jphotochemrev.2006.12.001

Brek, D. W. (1976). *Zeolite molecular sieves: structure, chemistry, and use.* Tarrytown, NY: Union Carbide Corporation.

Brites-Nóbrega, F. F., Polo, A. N. B., Benedetti, A. M., Leão, M. M. D., Slusarski-Santana V., & Fernandes-Machado, N. R. C. (2013). Evaluation of photocatalytic activities of supported catalysts on NaX zeolite or activated charcoal. *Journal Hazard Materials, 263*(Part 1), 61-66. doi: 10.1016/j.jhazmat.2013.07.061

Brites-Nóbrega, F. F., Santana, V. S., & Fernandes-Machado, N. R. C. (2011). Effect of support on the photocatalytic degradation of textile effluents using Nb2O5 and ZnO: photocatalytic degradation of textile dye. *Topics in Catalysis, 54*(1), 264-269. doi: 10.1007/s11244-011-9657-2

Brites-Nóbrega, F., Lacerda, I. A., Santos, S. V., Amorim, C. C., Santana, V. S., Fernandes-Machado, N. R. C., ... Leão, M. M. D. (2015). Synthesis and characterization of new NaX zeolite-supported Nb, Zn, and Fe photocatalysts activated by visible radiation for application in wastewater. *Catalysis Today, 240* (Part A), 168-175. doi: 10.1016/j.cattod.2014.06.036

Chong, M. N., Jing, B., Chow, C. W. K., & Saint, C. (2010). Recent developments in photocatalytic water treatment technology. *Water Research, 44*(10), 2997-3027. doi: 10.1016/j.watres.2010.02.039

Ejhieh, A. N., & Khorsandi, M. (2010). Photodecolorization of eriochrome black T using NiS–P zeolite as a heterogeneous catalyst. *Journal Hazard Mater, 176*(1-3), 629-637. doi: 10.1016/j.jhazmat.2009.11.077

Fan, J., Guo, Y., Wang, J., & Fan, M. (2009). Rapid decolorization of azo dye methyl orange in aqueous solution by nanoscale zerovalent iron particles. *Journal Hazard Mater, 166*(2-3), 904-910. doi: 10.1016/j.jhazmat.2008.11.091

Gaya, U. I., & Abdullah, A. H. (2008). Heterogeneous photocatalytic degradation of organic contaminants over titanium dioxide:a review of fundamentals, progress and problems. *Journal Photochem Photobiol C: Photochem, 9*(1), 1-12. doi: 10.1016/j.jphotochemrev.2007.12.003

Giannetto, P. G., Rendón, A. M., & Fuentes, G. R. (2000). *Zeolitas: características, propriedades y aplicaciones industriais* (2a ed.). Caracas, VE: Edditorial Innovación Tecnológica – Facultad de Ingenieria, UCV.

Gillman, G. P., & Uehara, G. (1980). Charge characteristics of soils with variable and permanent charge minerals: II. Experimental. *Soil Science Society of America Journal, 44*(2), 252-255. doi: 10.2136/sssaj1980.03615995004400020009x

Hadjltaief, H. B., Zina, M. B., Galvez, M. E., & Costa, P. (2016). Photocatalytic degradation of methyl green dye in aqueous solution over natural clay-supported ZnO–TiO2 catalysts. *Journal of Photochemistry and Photobiology A: Chemistry, 315*, 25-33. doi: 10.1016/j.jphotochem.2015.09.008

Kosinov, N., Auffret, C., Borghuis, G. J., Sripathi, V. G. P., & Hensen, E. J. M. (2015). Influence of the Si/Al ratio on the separation properties of SSZ-13 zeolite membranes. *Journal of Membrane Science, 484*, 140-145. doi: 10.1016/j.memsci.2015.02.044

Kosmulski, M. (2011). The pH-dependent surface charging and points of zero charge. V. Update. *Journal of Colloid and Interface Science, 353*(1), 1-15. doi: 10.1016/j.jcis.2010.08.023

Liotta, L. F., Gruttadauria, M., Di Carlo, G., Perrini, G., & Librando, V. (2009). Heterogeneous catalytic degradation of phenolic substrates: Catalysts activity. *Journal Hazard Mater, 162*(2-3), 588-606. doi: 10.1016/j.jhazmat.2008.05.115

Mohsin, M., Rasheed, A., Farooq, A., Ashraf, M., & Shah, A. (2013). Environment friendly finishing of sulphur, vat, direct and reactive dyed cotton fabric. *Journal of Cleaner Production, 53*, 341-347. doi: 10.1016/j.jclepro.2013.04.018

Nikazar, M., Gholivand, K., & Mahanpoor, K. (2008). Photocatalytic degradation of azo dye Acid Red 114 in water with TiO2 supported on clinoptilolite as a catalyst. *Desalination, 219*(1-3), 293-300. doi: 10.1016/j.desal.2007.02.035

Petkowicz, D. I., Pergher, S. B. C., Rochac, Z. N., & Santos, J. H. Z. (2010). Catalytic photodegradation of dyes by in situ zeolite-supported titania. *Chemical Engineering Journal, 158*(3), 505-512. doi: 10.1016/j.cej.2010.01.039

Prado, A. G. S., Bolzon, L. B., Pedroso, C. P., Moura, A. O., & Costa, L. L. (2008). Nb_2O_5 as efficient and recyclable photocatalyst for indigo carmine degradation. *Applied Catalysis B: Environmental, 82*(3-4), 219-224. doi: 10.1016/j.apcatb.2008.01.024

Schmal, M. (2011). *Catálise heterogênea*. Rio de Janeiro, RJ: Synergia.

Sędłak, A., & Janusz, W. (2008). Specific adsorption of carbonate ions at the zinc oxide/electrolyte solution interface. *Physicochemical Problems of Mineral Processing, 42*, 57-66.

Smith, B. (2003). Wastes from Textile Processing. In A. L. Andrady (Ed.), *Plastics and the Environment* (p. 293-295). doi: 10.1002/0471721557.ch7

Soon, A. N., & Hameed, B. H. (2011). Heterogeneous catalytic treatment of synthetic dyes in aqueous media using Fenton and photo-assisted Fenton process. *Desalination, 269*(1-3), 1-16. doi: 10.1016/j.desal.2010.11.002

Souza, R. P., Ambrosio, E., Souza, M. T. F., Freitas, T. K. F. S., Ferrari-Lima, A. M., & Garcia, J. C. (2017). Solar photocatalytic degradation of textile effluent with TiO2, ZnO, and Nb2O5 catalysts: assessment of photocatalytic activity and mineralization. *Environmental Science and Pollution Research, 24*(14), 12691-12699. doi: 10.1007/s11356-017-8408-8

Souza, R. P., Freitas, T. K. F. S., Domingues, F. S., Pezoti, O., Ambosio, E., Ferrari-Lima, A. M., & Garcia, J. C. (2016). Photocatalytic activity of TiO2, ZnO and Nb2O5 applied to degradation of textile wastewater. *Journal of Photochemistry and Photobiology A: Chemistry, 329*, 9-17. doi: 10.1016/j.jphotochem.2016.06.013

United Nations Educational, Scientific and Cultural Organization. (2015). *Scientific and cultural organization. Water for a sustainable world*. Paris, FR. Retrieved from https://www.unesco-ihe.org/sites/default/files/wwdr_2015.pdf